



Article

Cyanidin-3-*O*-glucoside Regulates the Expression of *Ucp1* in Brown Adipose Tissue by Activating *Prdm16* Gene

Suping Han ^{1,†}, Yafan Yang ^{1,†}, Yanan Lu ^{1,2,†}, Jielong Guo ¹, Xue Han ^{1,3}, Yunxiao Gao ¹, Weidong Huang ¹, Yilin You ^{1,*} and Jicheng Zhan ^{1,*}

¹ Beijing Key Laboratory of Viticulture and Enology, College of Food Science and Nutritional Engineering, China Agricultural University, Tsinghua East Road 17, Beijing 100083, China; hansuping@cau.edu.cn (S.H.); S20213061075@cau.edu.cn (Y.Y.); luyanan@bcu.edu.cn (Y.L.); b20183060515@cau.edu.cn (J.G.); hanxuehx313@bjmu.edu.cn (X.H.); s20193060991@cau.edu.cn (Y.G.); weidonghuang@cau.edu.cn (W.H.)

² School of Biomedicine, Beijing City University, Beijing 100094, China

³ Department of Physiology and Pathophysiology, School of Basic Medical Sciences, Peking University Health Science Center, Beijing 100191, China

* Correspondence: yilinyou@cau.edu.cn (Y.Y.); zhanjicheng@cau.edu.cn (J.Z.); Tel.: +86-10-62737535 (Y.Y.); +86-10-62737553 (J.Z.)

† These authors contributed equally to this work.

Abstract: (1) Background: Brown adipose tissue (BAT) burns energy to produce heat. Cyanidin-3-*O*-glucoside (C3G) can then enhance the thermogenic ability of BAT in vivo. However, the mechanism by which C3G regulates *Ucp1* protein expression remains unclear. (2) Methods: In this study, C3H10T12 brown adipose cells and db/db mice and mice with high-fat, high-fructose, diet-induced obesity were used as the model to explore the effect of C3G on the expression of the *Ucp1* gene. Furthermore, the 293T cell line was used for an in vitro cell transgene, a double luciferase reporting system, and yeast single hybridization to explore the mechanism of C3G in regulating *Ucp1* protein. (3) Results: we identified that, under the influence of C3G, *Prdm16* directly binds to the –500 to –150 bp promoter region of *Ucp1* to activate its transcription and, thus, facilitate BAT programming. (4) Conclusions: This study clarified the mechanism by which C3G regulates the expression of the *Ucp1* gene of brown fat to a certain extent.

Keywords: brown adipose tissue; Cyanidin-3-*O*-glucoside; PR domain containing 16; *Ucp1* promoter; peroxisomes proliferator-activated receptors



Citation: Han, S.; Yang, Y.; Lu, Y.; Guo, J.; Han, X.; Gao, Y.; Huang, W.; You, Y.; Zhan, J.

Cyanidin-3-*O*-glucoside Regulates the Expression of *Ucp1* in Brown Adipose Tissue by Activating *Prdm16* Gene. *Antioxidants* **2021**, *10*, 1986. <https://doi.org/10.3390/antiox10121986>

Academic Editor: Marco G. Alves

Received: 1 December 2021

Accepted: 8 December 2021

Published: 14 December 2021

Publisher's Note: MDPI stays neutral with regard to jurisdictional claims in published maps and institutional affiliations.



Copyright: © 2021 by the authors. Licensee MDPI, Basel, Switzerland. This article is an open access article distributed under the terms and conditions of the Creative Commons Attribution (CC BY) license (<https://creativecommons.org/licenses/by/4.0/>).

1. Introduction

Anthocyanins are polyphenolic compounds that are abundant in dark-colored fruits, vegetables, and pigmented cereals (such as berries, cherries, grapes, purple onions, black beans, purple cabbage, black rice, red sorghum, and purple maize (In addition, anthocyanins are commonly processed as colorants in beverages, fruit fillings, snacks, and dairy products, which account for a considerable amount of the anthocyanins consumed in the average diet [1]. Anthocyanin is a common component in functional foods for preventing cardiovascular diseases and inflammatory diseases (including diabetes and metabolic syndrome), mainly due to its excellent antioxidant activity [2]. In anthocyanin-related structures, the carboxypyranoside -3-*O*-glucoside, in particular, exhibits a good inhibition effect on active oxygen generation and high structural stability [3]. A large number of studies have proven that anthocyanins offer a variety of therapeutic effects, including that of increased energy expenditure and of limiting weight gain provided by Cyanidin-3-*O*-glucoside (C3G) [4].

The rising prevalence of excess body mass and obesity in nearly all countries around the world has been described as a global pandemic [5]. Currently available anti-obesity strategies are largely dependent on limiting energy uptake and/or absorption, but these tend to have little effect and often cause unwanted side effects [6,7]. An alternative strategy

is urgently required to increase the energy expenditure in key metabolic organs, such as brown adipose tissue (BAT) [8]. In rodents, increasing BAT activity can effectively enhance metabolic rate and protect the animal from obesity [9].

BAT plays an essential role in non-shivering thermogenesis in mammals. Its cells are rich in mitochondria, the inner membranes of which are, in turn, rich in uncoupling protein 1 (Ucp1). BAT can specifically overexpress Ucp1, thus uncoupling transmembrane electron transfer and oxidative phosphorylation in the mitochondrial respiratory chain, thereby releasing a large amount of energy in the form of heat [10]. The known anti-obesity effect of functional BAT has drawn research and attention to the activation and regulation mechanism of brown fat functioning, and the specific expression of Ucp1 by BAT has become a hot topic for scientists.

The expression of the *Ucp1* gene is regulated by a variety of transcription factors, such as peroxisome proliferator-activated receptors (PPARs), PR domain containing 16 (Prdm16), peroxisome proliferator-activated receptor γ coactivator-1 (PGC-1), and mitochondrial transcription factor A (TFAM). PPAR α participates in the regulation of fatty acid oxidation mainly by inducing the expression of genes related to fatty acid oxidation [11]. Prdm16 is a zinc finger structure transcription factor containing PR domain, which is highly expressed in mouse BAT. It is also a key factor in determining whether adipose precursor cells develop into skeletal muscle cells or brown adipose cells. The Prdm16 protein is greatly enriched in BAT and causes increased expression of mitochondrial genes and greater density of mitochondria [12]. The loss of Prdm16 can hinder the differentiation of brown adipocytes, while overexpression can significantly increase their numbers. Animals lacking Prdm16 in BAT have a dramatically reduced capacity to produce heat [13]. Prdm16 regulates the thermogenic function of brown fat, mainly by binding to PPAR γ and coactivating its transcriptional function [14].

The anti-obesity and anti-diabetic effects of anthocyanins are well-accepted experimentally [15,16]. Anthocyanins C3G and C3R have been reported to increase the mitochondrial copy number in vitro and to promote the metabolism of carbohydrates and fat [17]. C3G can enhance whole-body metabolism by upregulating the mitochondrial function of BATT and beige formation in subcutaneous WAT [4]. However, its molecular targets have yet to be elucidated.

Here, via quantitative real-time PCR, to quantify the expression of BAT-related genes *Ucp1* and *Prdm16* following the treatment of C₃H₁₀T_{1/2} cells with C3G during brown adipogenesis, we speculate that *Prdm16* may be a novel transcriptional activator of *Ucp1*. The results of a luciferase assay and yeast one-hybrid screening ascertained that C3G activates the thermogenic gene *Ucp1* by regulating the expressions of *Prdm16*. Thus, Prdm16 can bind directly to the *Ucp1* promoter region, from -500 to -150 bp to active transcription. Our results, thus, suggest that Prdm16 is indeed a novel transcriptional activator of *Ucp1* and that C3G can increase energy metabolism through a previously unrecognized molecular mechanism. Consequently, these findings may support an innovative approach to the treatment of obesity and its related diseases.

2. Materials and Methods

2.1. Materials and Reagents

C3G (purity 95.7%) was purchased from Chengdu Manchester Co., Ltd. (Chengdu, China), A ready-to-use PCR kit 3.0 was purchased from Beijing Tianenze Biotechnology Co., Ltd. (Beijing, China), which is used for PCR identification of bacterial liquid, and the method is carried out according to the instruction manual. Dimethyl sulfoxide (DMSO), a double luciferase reporter gene detection kit, and Lipo8000TM transfection reagent were purchased from Beyotime Biotechnology Co., Ltd. (Shanghai, China), while a HiFi Script cDNA Synthesis Kit, Ultra SYBR Mixture, and 200 bp Ladder DNA Marker were purchased from Kangwei Century Biology Science and Technology Co., Ltd. (Beijing, China), and a mass extraction and purification kit for plasmid was purchased from Weigela Biology

Technology Co., Ltd. (Chengdu, China). Furthermore, recombinant human PPARA (P0645) was purchased from Wuhan Fine Biotechnology Co., Ltd. (Wuhan, China).

2.2. Cell Culture

The mouse mesenchymal stem cell line, known as C₃H₁₀T_{1/2} mouse embryonic fibroblasts, was purchased from the cell bank of the Chinese Academy of Sciences (Shanghai, China), and was induced to differentiate into brown adipocytes. The C₃H₁₀T_{1/2} cells used in this experiment were cell samples frozen in liquid nitrogen in the laboratory.

The cryovials were taken out of the liquid nitrogen and immediately melted in a 37 °C water bath, centrifuged at 500 × g for 3 min, and cultured in a 37 °C, 5% CO₂ incubator for passage. When the cells grew to a density of 80–90%, the medium was changed to brown adipose differentiation medium (DMEM HIGH + 10% FBS + 0.02 μM INSULIN + 1 × 10^{−3} μM T3) and an appropriate concentration of C3G was added. Two days later (recorded as day 0), the medium was changed to brown fat induction medium (DMEM HIGH + 10% FBS + 0.02 μM INSULIN + 1 × 10^{−3} μM T3 + 0.125 mM INDOMETHACIN + 0.5 mM IBMX + 2 μg/mL DEX) and an appropriate concentration of C3G was added. Two days later (recorded as day 2), the medium was changed to the brown adipose differentiation medium described above, and an appropriate concentration of C3G was added. The liquid was changed again on the 4th day. On the sixth day, the cells were observed under an inverted microscope. There were obvious fat droplets in the cytoplasm, i.e., the differentiation was completed.

2.3. Animals Studies

Animal experiments were conducted according to the methods reported by You et al. [4,18]. Animal experiments were conducted in two stages. Firstly, 20 three-week-old obese C57BLKS/J-Leprdb/Leprdb (db/db) male mice (mouse model of hereditary obesity) were purchased from the Model Animal Research Center of Nanjing University, China. After an acclimation of one week, the mice were randomly divided into two groups ($n = 10$ per group) with overall equal body weights. The mice received C3G (1 mg/mL) dissolved in drinking water for 12 weeks. DMSO was used as the vehicle for different treatments. In addition, a further 36 three-week-old male C57BL/6J mice (obesity model mice induced by high fat and high glucose diet) were purchased from Vital River Laboratory Animal Technology Co., Ltd., China. After one week of acclimation, these mice were randomly divided into three groups ($n = 12$ /group) with overall equal body weights. They were assigned to one of three dietary treatments for 12 weeks: (1) normal chow diet group (CHOW, 3.2 kcal/g, 4.5% fat, w/w); (2) diet-induced obesity group (DIO, 4.7 kcal/g, 25% fructose and 25% lard); and (3) C3G group (DIO + C3G, 4.7 kcal/g, 25% fructose and 25% lard). C3G-group mice received C3G dissolved in drinking water (1 mg/mL), while drinking water also served as the vehicle for the CHOW and DIO treatments. Three mice were housed per cage in an Office of Laboratory Animal Welfare-certified animal facility, with a 12-h light/12-h dark cycle. Principles of laboratory animal care were followed, with all procedures conducted according to the guidelines established by the National Institute of Health, and every effort was made to minimize suffering.

2.4. Isolation of Total RNA Extraction and Analysis by qPCR

The total RNA of cells and BAT were extracted using RNAiso Plus reagent. Isolated RNA was quantified by measuring optical density (OD) at 260 and 280 nm with a NanoDrop 2000 spectrophotometer (Thermo Scientific, Waltham, MA, USA). The cDNA was synthesized by means of a PrimeScript RT reagent kit (Takara Biotechnology Co., Ltd., Dalian, China) and the assay was performed using real-time PCR with a SYBR Premix Ex Taq™ I and 7500 Real-Time PCR System (Applied Biosystems, Foster City, CA, USA). Data were normalized to the internal control actin and analyzed using the $\Delta\Delta C_t$ method. Primer sequences for the *Ucp1* promoter and *Prdm16* are listed in Table 1.

Table 1. Primer sequences used for qRT-PCR.

Gene	Primer Sequence (5'→3')
<i>Ucp1</i>	F:GGCAAAAACAGAAGGATTGC R:TAAGCCGGCTGAGATCTTGT
<i>Prdm16</i>	F:GAAGTCACAGGAGGACACGGR: CTCGCTCCTCAACACACCTC

2.5. Construction of Plasmid Vector

The primers were designed and cloned according to the selected gene fragments, and the target gene was recombined with the vector and transformed into *E. coli*. Thereafter, PCR and double enzyme digestion were performed, followed by sequencing for identification, and the detected correct plasmid vector was used for subsequent experiments. The cleavage sites and vector plasmids of the different gene fragments involved in this experiment are shown in Table 2.

Table 2. The cleavage sites and vector plasmids of the different gene fragments.

Vector	Gene	Primer Sequence (5'→3')
Double luciferase reporter gene vector of <i>Ucp1</i> promoter	<i>Ucp1</i> -Kpn I-F <i>Ucp1</i> -Mlu I-R	GGGGTACCcattctctaagaccatagctt CGACGCGTacttctgcgcctgacct
Eukaryotic vector for overexpression of <i>Prdm16</i>	<i>Prdm16</i> -EcoRI-F <i>Prdm16</i> -XbaI-R	tccaagcttctgcaggaattcA TGCGA TCCAAGGCGAGG accgggccactagttctagaTCA TTGCA TA TGCCTCCGGG
Double luciferase reporter gene vector of <i>Ucp1</i> promoter with different fragment size	<i>Ucp1</i> (-150bp)-Kpn I-F <i>Ucp1</i> (-150bp)-Mlu I-R <i>Ucp1</i> (-500bp)-Kpn I-F <i>Ucp1</i> (-500bp)-Mlu I-R <i>Ucp1</i> (-1000bp)-Kpn I-F <i>Ucp1</i> (-1000bp)-Mlu I-R <i>Ucp1</i> (-1500bp)-Kpn I-F <i>Ucp1</i> (-1500bp)-Mlu I-R	atttctctatcgataggtaccGAGTGACGCGCGGCTGGG cgagccgggctagcagcgtCTGCGCCCTGACCTGGGA atttctctatcgataggtaccTCCAGTCAACCAAA TCTGAAGG cgagccgggctagcagcgtCTGCGCCCTGACCTGGGA atttctctatcgataggtaccAGCAGAACCCTGGCCAACCA cgagccgggctagcagcgtCTGCGCCCTGACCTGGGA atttctctatcgataggtaccTATTATACTGTTGTTGCTGCTGCT cgagccgggctagcagcgtCTGCGCCCTGACCTGGGA
pLacZi- <i>Ucp1</i>	<i>Ucp1</i> -EcoR I-F <i>Ucp1</i> -Xho I-R <i>Prdm16</i> -EcoR I-F <i>Prdm16</i> -Xho I-R	ctttgatattggatcgaattcCATTCTCTAAGACCATAGCTTGGT atacagagcacatgctcagACTTCTGCGCCCTGACCTG gattatgcctctcccgaattcTACGCTAGGTTCCGCTCCC agaagtccaagcttctcgagTAGTAACGTA TACGGAGGCCCA T
PJG- <i>Prdm16</i>	<i>Prdm16</i> -EcoR I-F <i>Prdm16</i> -Xho I-R	gattatgcctctcccgaattcTACGCTAGGTTCCGCTCCC agaagtccaagcttctcgagTAGTAACGTA TACGGAGGCCCA T

The primer sequence was designed by CE Design, via the official website of Nanjing Vazyme Biotechnology Co., Ltd. (Nanjing, China), (www.vazyme.com (accessed on 31 May 2020)), according to the gene sequence provided by NCBI, and the primer was synthesized by Shanghai Sangon Biological Engineering Technology Co., Ltd. (Shanghai, China).

2.6. Cell Transfection and Luciferase Activity Detection

Cell transfection was performed using the method described in the Lipo8000 Transfection Reagent, Beyotime Biotechnology, Inc., with some modification. The transfection reagent was configured to 50 µL of Opti-MEM® (Thermo Scientific, Waltham, MA, USA) Medium, 1 µg of plasmid DNA, and 1.6 µL of Lipo8000™ (Beyotime Biotechnology, Shanghai, China) transfection reagent. After 24 h transfection, the cells were lysed, and firefly luciferase detection reagent and renal luciferase detection working solution were added, respectively, to measure RLU on a multifunctional microplate reader.

2.7. Yeast One-Hybrid Assay

In order to verify the interaction between *Prdm16* and the *Ucp1* promoter, in this experiment, the *pLacZi-Ucp1* reporter vector and *pJG-Prdm16* fusion expression vector were constructed and transfected into yeast to screen for blue leukoplakia.

Respectively, the *Prdm16* was connected with the PJG plasmid after enzyme digestion, the *Ucp1* promoter was connected with the *pLacZi* plasmid after enzyme digestion, and co-transfection was performed into EGY48 competent cells. The cells transfected with Placezi+ and PJG+ were used as the positive control, *pLacZi-Ucp1* and PJG empty vectors were used as the self-activated control, and the Placezi empty vector and *pJG-Prdm16* were used as the negative control. The cells were cultured in a SD-trp/ura-deficient medium for 48 h, after which single colonies were picked and cultured in X- α -gal medium for 48 h, and the results were observed.

2.8. shRNA-Mediated Gene Silencing of *Prdm16*

According to the gene sequence number information provided by NCBI, a primer sequence was designed through the GPP Web Portal website: 5'-CCGGGACGGTGACGTTGTAAATAATCTCGAGATTATTTACAACGTCACCGTCTTTTTG-3'. The pLKO.1 vector was enzymatically cleaved with AgeI (NEB, #R0552S) and EcoRI (NEB, #R0101S) for ligation and transformation. The collected plasmids were transferred into C₃H₁₀T_{1/2} cells and inoculated onto a 6-well cell culture plate. After further differentiation for 6 days, according to the brown adipose differentiation method, the mRNA expressions of *prdm16* and *Ucp1* mRNA the cells were detected by RT-PCR.

2.9. Microscale Thermophoresis (MST) Study

The MST micro-thermophorescope (Monolith NT.115) was derived from Northrop. First, the PPAR α protein was fluorescently labeled to make it become a reporter molecule, and the gradient-diluted C3G molecule was mixed with the PPAR α protein of the same concentration in an equal amount and loaded into the capillary. The affinity of molecular interactions was quantitatively analyzed by detecting the fluorescence changes caused by thermophoresis in capillaries with different concentrations under the temperature gradient field. The experimental results were automatically analyzed by MO Affinity Analysis software, and the K_d value was calculated accurately.

2.10. Analysis of Experimental Data

All data were expressed as means \pm SD. Statistical analysis was conducted using GraphPad Prism (version 7.0). The statistical differences between the groups were evaluated using one-way ANOVA with a least significant difference (LSD) test, and a *p*-value less than 0.05 was considered statistically significant.

3. Results

3.1. C3G Upregulates the Expression of *Ucp1* Gene Both In Vitro and In Vivo

As mentioned above, it has previously been reported that C3G treatment specifically upregulates the thermogenic gene expressions in BAT-cMyc cells [17]. In this study, we treated C₃H₁₀T_{1/2} cells with various concentrations of C3G to explore the effect of C3G on the expression of the *Ucp1* gene. However, this proved to have no effect on BAT-cMyc cell viability or proliferation during brown adipogenesis. In comparison with the PBS medium, C3G at concentrations of 10 μ M, 20 μ M, and 40 μ M was found to significantly upregulate the relative expression level of *Ucp1* mRNA in the C₃H₁₀T_{1/2} cells (*p* < 0.05) and, at 20 μ M, the C3G could significantly upregulate the expression of *Ucp1* (Figure 1A) (*p* < 0.01). Similarly, through the animal experiments, it was found that C3G treatment could significantly increase the expression of the *Ucp1* gene of BAT in db/db mice and mice with DIO. The expression of *Ucp1* in the C3G-treated mice was 3.82 times and 3.06 times higher than those in the two control groups (Figure 1B,C). These results are consistent with

our previous research results [4,17], further demonstrating C3G-induced upregulation of *Ucp1* mRNA expression, both in vitro and in vivo.

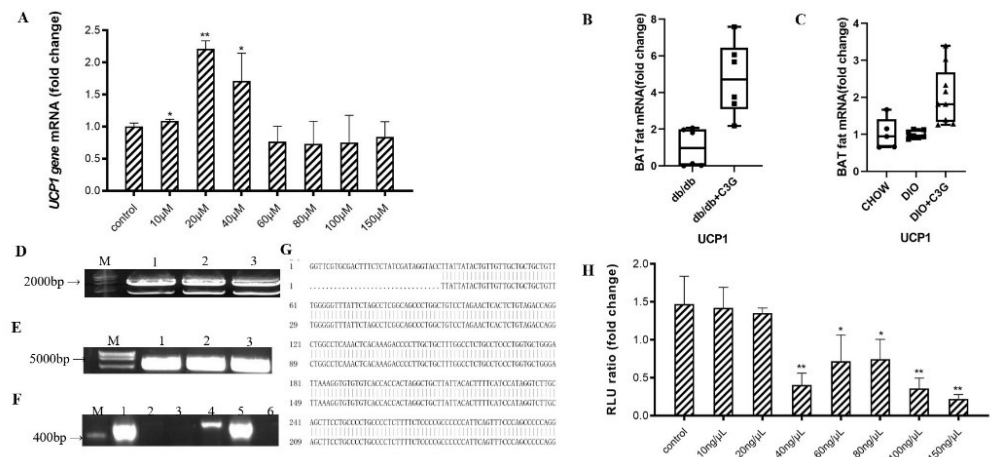


Figure 1. C3G was able to up-regulate the expression of *Ucp1* gene both in vitro and in vivo. (A) Effects of C3G at different concentrations on *Ucp1* gene expression in C₃H₁₀T_{1/2} cells. (B,C) C3G up-regulated the expression of *Ucp1* gene both in db/db mice model (B) and mice with DIO model (C) ($n = 6-8$). (D) Electrophoretic map of cloned *Ucp1*, M: Kang was 200Bpladder; Lane 1–3: *Ucp1* amplification products (E) Electrophoresis diagram of pGL3-Basic enzyme digestion product, M: DL15000 marker; Lane 1–3: pGL3-Basic double enzyme digestion product. (F) PCR electrophoresis diagram of pGL3-*Ucp1* bacterial solution; M: Kang Wei 200Bpladder; Lane 1–6: PCR products from the picked six single-colony bacterial solutions. (G) Comparative diagram of sequencing results of PGL3-*Ucp1* (H) Activation of *Ucp1* promoter by C3G with different concentrations. Values represent means \pm SD. Error bars represent SD; mean values with asterisk or different letters are significantly different (* means $p < 0.05$; ** means $p < 0.01$).

All figures and tables should be cited in the main text as Figure 1, Table 1, etc.

Next, we successfully constructed the luciferase reporter gene vector (Figure 1D–G), to examine the role of C3G in the activation of *Ucp1*. The luciferase assay showed that, compared with the PBS-supplemented medium, treatments with various concentrations of C3G and transfection with the -2.0 kb *Ucp1* promoter–luciferase did not activate the *Ucp1* promoter (Figure 1H) ($p < 0.01$). Thus, these results indicate that, while C3G significantly accelerates *Ucp1* expression, it does not directly activate its promoter.

3.2. C3G Upregulates the Expression of *Prdm16* Gene Both In Vitro and In Vivo

As the expression level of the BAT-specific gene *Ucp1* was increased by C3G treatment and this process was not dependent on the activation of the *Ucp1* promoter, we speculated the existence of other regulators as target genes of C3G, such as transcription factors. *Prdm16* determines the brown fat-like program and thermogenesis in both brown and white adipose tissues [19–22], so we consequently sought to determine whether this thermogenesis-related gene participates in this process, and found that treatment with C3G (20 μ M) resulted in a 4.42-fold increase in *Prdm16* mRNA expression in C₃H₁₀T_{1/2} cells, compared to the control group. Interestingly, the expression levels of *Prdm16* followed the same trend as that of *Ucp1* after treatment with various concentrations of C3G (Figure 2A) ($p < 0.01$). Moreover, the promotional effect of C3G on *Prdm16* was consistent with that in previous reports [4,17]. Similarly, in light of the animal experiments in this study, it was ascertained that C3G treatment can significantly increase the expression of *Prdm16* and *PPAR α* genes in the BAT of mice. In the db/db mouse model and the DIO model mice, the expressions of *Prdm16* and *PPAR α* genes in C3G-treated mice increased by 7.21 times, 10.16 times, 3.91 times, and 4.58 times ($p < 0.05$), respectively, compared with the control group (Figure 2B,C). These results are consistent with our previous research results [4,17],

indicating clearly that C3G treatment increased the expression of *Prdm16* gene, both in vitro and in vivo.

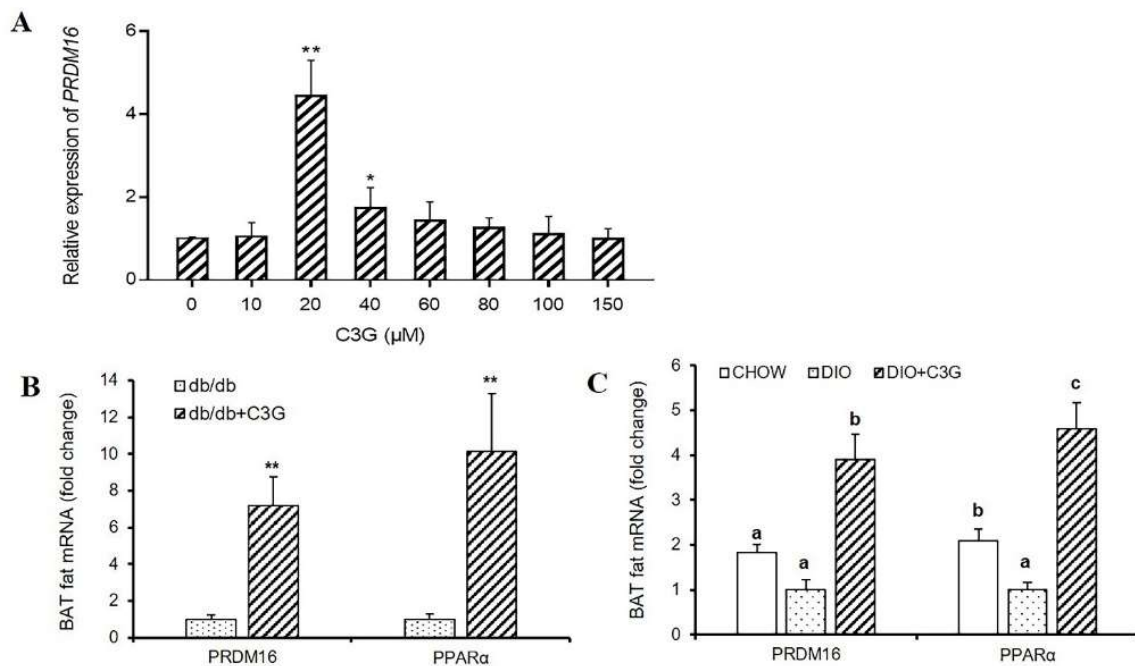


Figure 2. C3G was able to up-regulate the expression of *Prdm16* gene both in vitro and in vivo. (A) Effect of C3G at different concentrations on *Prdm16* gene expression in C3H10T12 cells. (B,C) Gene expression profile in BAT, real-time PCR analysis of thermogenic-related genes, including *Prdm16*, PPARα in db/db mice model (B) and mice with DIO model (C) ($n = 6-8$). Values represent means SD. Error bars represent SD; mean values with asterisk or different letters are significantly different (* means $p < 0.05$; ** means $p < 0.01$).

3.3. *Prdm16* Regulates the Expression of *Ucp1* Gene in Brown Adipocytes

We hypothesized accordingly that C3G may first upregulate the expression of gene *Prdm16* and then activate *Ucp1*. To explore and examine the effect of transcription factor *Prdm16* on *Ucp1* expression, we constructed a *pCMV-Prdm16* vector to transfect $C_3H_{10}T_{1/2}$ cells and further ascertained the level of *Ucp1* mRNA via quantitative real-time PCR after the completion of adipocyte differentiation (Figure 3A–C). As expected, *Prdm16* did regulate *Ucp1* expression at the level of transcription. In the treatment group in which *Prdm16* was overexpressed, the expression of *Ucp1* increased over four times more than that in the control group, with a significant up-regulation effect (Figure 3D) ($p < 0.01$). Further, to validate the loss-of-function studies, we constructed shPRDM16 to transfect $C_3H_{10}T_{1/2}$ cells and further determine *Ucp1* mRNA levels by quantitative real-time polymerase chain reaction after adipocyte differentiation. As shown in Figure 3E, shPRDM16 reduced *Ucp1* expression at the transcriptional level by more than 0.5 times that of the control group. Taken together, these results indicate that C3G did, at least partly, activate *Ucp1* by regulating the expression of the transcription factor *Prdm16*.

3.4. *Prdm16* Directly Binds and Activates *Ucp1* Promoter

As a transcription factor, *Prdm16* often regulates gene expression by binding to the promoter region of the target gene. To determine the mechanism by which *Prdm16* regulates *Ucp1*, we performed a double luciferase reporter experiment to quantitate promoter activation. Compared to the empty vector control, co-transfection of *pCMV-Prdm16* with the -2.0 kb *Ucp1* promoter–luciferase resulted in an obvious activation of the *Ucp1* promoter (Figure 4A) ($p < 0.01$).

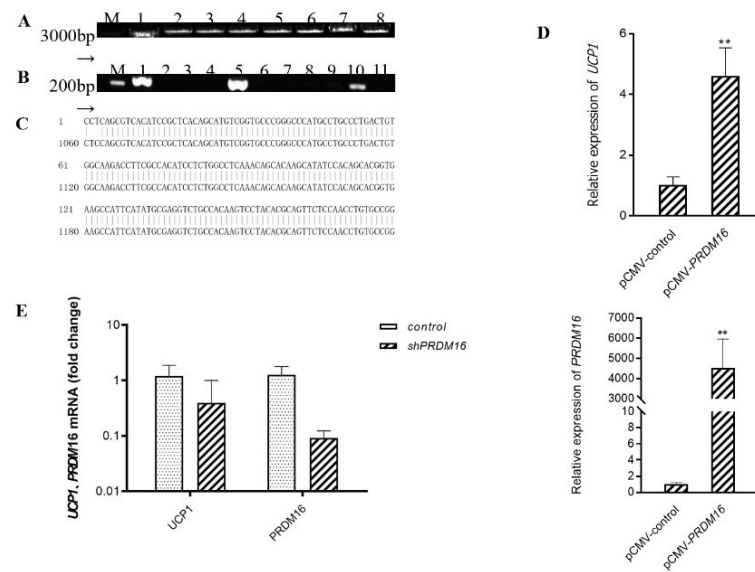


Figure 3. Overexpression of *Prdm16* upregulates *Ucp1* gene expression in brown adipose cells (A) Clone *Prdm16* electrophoretic map, M: Kang Wei 200B PLA DD; Lane 1–8: *Prdm16* amplification product. (B) PCR electrophoresis diagram of pCMV-Prdm16 bacterial solution; M: Kang Wei 200B PLA DD; Lane 1–11: PCR products from the picked bacterial solutions of 11 single colonies. (C) Comparative diagram of pCMV-Prdm16 sequencing results. (D) Effect of overexpression of *Prdm16* on *Ucp1* gene expression C3H10T12 cells. (E) Effects of shPRDM16 on *Ucp1* gene expression during C₃H₁₀T_{1/2} cell differentiation. Compared with control, ** means $p < 0.01$.

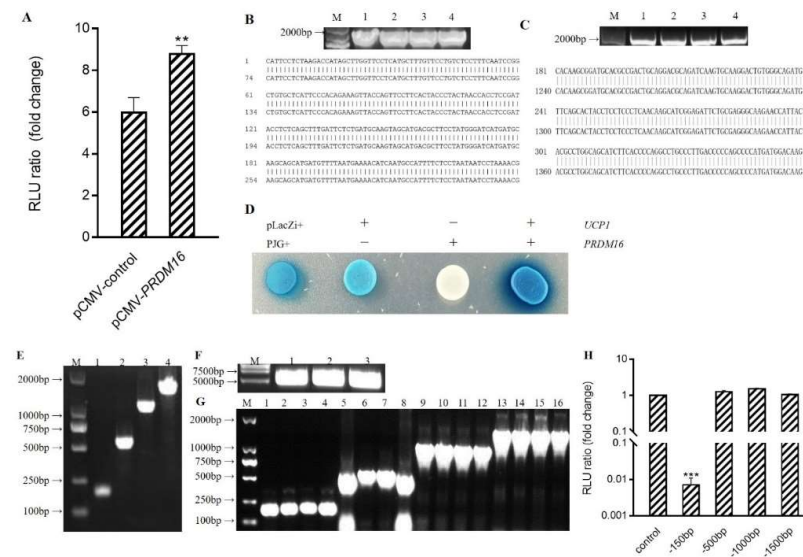


Figure 4. *Prdm16* capable of activating *Ucp1* promoter (A) Effect of *Prdm16* on *Ucp1* promoter (double luciferase report gene method) (B) PCR electrophoresis diagram and sequencing comparison diagram of pLacZi-*Ucp1* bacterial solution. M: Kang Wei 200B PLA DD; Lane 1–4: PCR products from the picked four single-colony bacterial solutions. (C) PCR electrophoresis diagram and sequencing comparison diagram of pJG-*Prdm16* bacterial solution. M: Kang Wei 200B PLA DD; Lane 1–4: PCR products from the picked four single-colony bacterial solutions. (D) Effect of *Prdm16* on *Ucp1* promoter (yeast one-hybrid assay) (E) Clone electrophoretic images of *Ucp1* promoter with different lengths. (F) PGL3-Basic enzyme digestion electrophoresis diagram (G) PCR electrophoresis map of bacterial solution after ligation of *Ucp1* promoter with different lengths to pGL3-Basic. (H) Effects of *Prdm16* on promoters of different fragments *Ucp1*. Compared with control, ** means $p < 0.01$; *** means $p < 0.001$.

This interaction of *Prdm16* with the *Ucp1* promoter was subsequently verified. A *pLacZi-Ucp1* reporter vector and *pJG-Prdm16* fusion expression vector were constructed and transfected into yeast for blue-streak screening (Figure 4B–D). Similar to the positive control group of Plazzi+ and PJG+, treatment groups transfected with *pLacZi-Ucp1* and *pJG-Prdm16* were blue and dark in color. The results verified by the single yeast hybrid assay showed that *Prdm16* could directly bind to the *Ucp1* promoter.

To start defining how *Prdm16* activates the *Ucp1* promoter, 5' deletions of the *Ucp1* promoters driving a luciferase reporter were generated and co-transfected along with *pCMV-Prdm16* into 293 cells (Figure 4E–G). All *Ucp1* promoter constructs deleted down to –500 bp, thus showing remarkable activation upon *Prdm16* co-transfection. However, *Ucp1* promoter activation by *Prdm16* was lost when the promoter was deleted to –150 bp, indicating that *Prdm16* functions through the sequence from –500 to –150 bp (Figure 4H).

3.5. PPAR α Binds to *Ucp1* Promoter to Activate Transcription

The above experiments showed that *Prdm16*, regulated by C3G, plays a novel role in upregulating the expression of *Ucp1*; however, it has been previously reported that the expression of *Ucp1* is regulated by many factors. We found that *PPAR α* , a gene associated with fatty acid oxidation, could also activate *Ucp1* promotion in the same way as *Prdm16* (Figure 5A–E) ($p < 0.01$). In addition, the results of the luciferase activity assay showed that the activity of the –150 bp *Ucp1* promoter was significantly reduced (Figure 5F) ($p < 0.01$). Analysis, combined with the results of this assay, showed that the region where the *Ucp1* promoter binds to *PPAR α* is between –500 and –150 bp upstream of its initiation site.

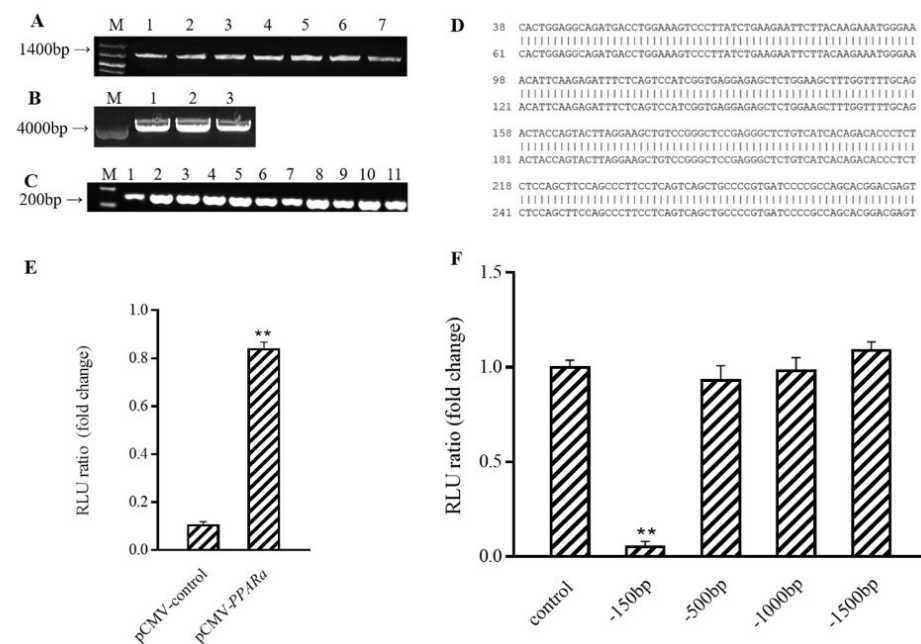


Figure 5. PPAR α binds to *Ucp1* promoter to activate transcription. (A) Cloned PPAR α electrophoresis M: Kang Wei 200B PLA DD; Lane 1–7: PPAR α amplification product. (B) Electrophoresis map of pCMV-N-Flag enzyme digestion product, M: Kang Wei 200B PLA DD; Lane 1–3: pCMV-N-Flag double enzyme digestion product. (C) PCR electrophoresis diagram of pCMV-PPAR α bacterial solution; M: Kang Wei 200B PLA DD; Lane 1–11: PCR products from picked 11 single-colony bacterial solutions (D) Comparison of pCMV-PPAR α sequencing results. (E) Effect of PPAR α on the intact *Ucp1* promoter (–2000 bp). (F) Effect of PPAR α on promoter of *Ucp1* with different fragments. ** mesns $p < 0.01$.

3.6. Conformational Investigation and Interaction Study of PPAR α –C3G

Molecular modeling of the PyMOL program was used to improve understanding of the PPAR α –C3G interaction. The optimal energy sequencing results for PPAR α and

thereby dissipating the electrochemical gradient normally used for ATP synthesis [29]. The regulation of levels of the *Ucp1* gene, thus, plays a decisive role in the control of *Ucp1* content and is at the center of the physiological regulation of BAT heat production [30]. Revealing the involved signal pathway and transcription regulation of *Ucp1* in BAT's energy metabolic process not only helps us to better understand the important role of *Ucp1* in BAT energy metabolism control but also provides a theoretical foundation for obesity treatment based on BAT.

Our previous research showed that dietary supplementation with the functional ingredients of natural plants exhibited a positive effect on BAT functionality in mice. Such plant-based ingredients include mulberry polyphenol extract, such as C3G and rutin [4,18,31]. Moreover, some phenolic acids, such as vanillic acid and chlorogenic acid, which are components of mulberry fruit polyphenols, also induce the thermogenesis of BAT and could, therefore, be applied to the prevention of dietary-induced obesity and insulin resistance [31,32]. We previously reported that mulberry and mulberry wine extract (ME and MWE) can not only improve the expression of BAT specific gene *Ucp1*, but also improve the mitochondrial copy number [33]. As the most abundant anthocyanin in ME and MWE, C3G has also been proven to increase the quantity of mitochondria in subsequent experiments [17]. In order to further explore the heat production mechanism of BAT promoted by C3G, we studied the mitochondrial biogenesis and function. The results show that C3G significantly upregulated the expression of mitochondrial synthesis-related genes *Tfam*, *NRF1* and *NRF2*, in both the BAT of both the db/db and mice with DIO, and increased the number of mitochondria and the expression levels of mitochondrial oxidative phosphorylation-related proteins ATP5A, UQCRC2, and NDUFB8 [4,18].

This strongly suggested the promotion of BAT heat production by C3G, thus warranting further exploration of the mechanism by which C3G regulates the action of *Ucp1* and its related heat production gene. In this study, we first verified the promotional effect of C3G on *Ucp1* gene expression through animal models. Thereafter, we found that C3G can upregulate the BAT specific gene *Ucp1* expression during brown adipocyte differentiation, thereby effectively increasing the mitochondrial respiration uncoupling of brown adipocytes, which is consistent with the previously reported conclusion [34]. However, our study found that there is no concentration dependence, and also that the activation of *Ucp1* by C3G is not achieved by activating the promoter, thus suggesting the existence of other regulatory factors in the process.

Numerous studies have shown that the activity of *Ucp1* is inhibited by nucleotides and activated by non-lipidated fatty acids [33,35]. Norepinephrine (NE) released by sympathetic nerves or hypothermia are the main physiological signals that activate *Ucp1* synthesis in BAT cells [36]. Furthermore, the synthesis of *Ucp1* is strongly regulated by the transcription level; cAMP is the main activator of *Ucp1* gene transcription [37–40]; and β 3-AR-specific agonists L-755507, CGP12177, CL316243, and BRL35135 can significantly increase the levels of *Ucp1* mRNA in mammalian BAT cells [38–40]. In addition, several transcription factors and coregulators found in both WAT and BAT, as well as in other tissues, including PPARs, PGC1 α , and ATF2, have been implicated in the transcriptional activation of *Ucp1* [12,41]. Our data show that C3G can activate *Ucp1* by upregulating the expression of the transcription factor *Prdm16*. Since *Prdm16* is related to heat production [42,43], it is even clearer that C3G does indeed play a role in weight loss by activating heat production.

Prdm16 can form transcription complexes with other transcription factors, such as C/EBP β , PGC1 α , PPAR α , and PPAR γ , to regulate the expression of thermogenic genes [14,44]. Furthermore, it was found in our previous research that C3G can upregulate PPAR α [4]. Consequently, on the basis of the above discussion, it would be reasonable to believe that PPAR α is also involved in *Ucp1* transcriptional regulation. Through double luciferase experiments, we ascertained that PPAR α can indeed activate the transcriptional expression of *Ucp1* in a similar manner to that of *Prdm16*. Unlike *Prdm16*, however, PPAR α is a fatty acid oxidation-related gene that is also expressed in WAT, which suggests that

the transcriptional activation of C3G to *Ucp1* is not limited to BAT. C3G is expected to achieve weight loss and lipid reduction by increasing WAT heat production, which would be consistent with previous conclusions [18].

On the one hand, we proved that C3G could enhance the thermogenesis of BAT. On the other hand, anthocyanins were reported to have anti-cancer and anti-inflammatory effects [45], which were closely related to their antioxidant activities. Therefore, the role of antioxidant activity of C3G in thermogenesis could be further explored. However, there are a variety of metabolites of C3G, and 41 metabolites have been identified. Among them, protocatechuic acid and vanilloid are metabolites that exert the main physiological functions of C3G in the body [46]. For example, PCA and PGA, the degradation products of C3G, inhibit the proliferation of cancer cells, which is closely related to their antioxidant activity [47]. The effect of C3G on the thermogenesis of brown fat suggests that its metabolites may have the same effect or even more obvious effects. Therefore, the above C3G metabolites can be further studied in future studies to further clarify the effective activators that activate *Ucp1*.

5. Conclusions

Taken together, the findings of our study indicate that C3G can upregulate the expression level of *Prdm16*, and then activate the transcriptional expression of *Ucp1* by directly binding to the -500 to -150 bp region of the *Ucp1* promoter.

In future research, it would be valuable to determine whether *Prdm16* interacts with PPAR α or other activating factors to activate *Ucp1* and to determine the molecular mechanism by which C3G regulates *Prdm16* expression. The results of this study provide an effective approach for the development of novel methods to improve energy metabolism with the activation of *Ucp1* as the target, and also help to establish an innovative theoretical basis for the in-depth utilization and development of C3G-rich fruit and vegetable resources.

Author Contributions: Conceptualization, Y.Y. (Yilin You) and J.Z.; methodology, W.H.; software, J.G.; validation, Y.Y. (Yafan Yang), S.H. and Y.L.; formal analysis, X.H.; investigation, Y.G.; resources, Y.Y. (Yilin You); data curation, Y.Y. (Yilin You); writing—original draft preparation, Y.Y. (Yafan Yang) and S.H.; writing—S.H. and Y.L.; visualization, S.H.; supervision, Y.Y. (Yilin You); project administration, J.Z.; funding acquisition, Y.Y. (Yilin You). All authors have read and agreed to the published version of the manuscript.

Funding: This research was funded by the National Natural Science Foundation of China Youth Fund (81900777) to Yilin You and the National “Thirteenth Five-Year” Plan for Science and Technology Support (2016YFD0400500) to Weidong Huang.

Institutional Review Board Statement: This study was approved by the Animal Experiment Committee of the College of Food Science and Nutritional Engineering, China Agricultural University (authorization reference number CFSNE20190038).

Informed Consent Statement: Not applicable.

Data Availability Statement: The data presented in this study are available in this manuscript.

Conflicts of Interest: The authors declare no conflict of interest.

References

1. You, Y.; Zhou, F.; Huang, D. Eating the Right Color: Dietary Anthocyanins and Obesity Control. *Food Beverage Asia* **2018**, *12*, 57–59.
2. Duchowicz, P.R.; Szewczuk, N.A.; Pomilio, A.B. QSAR Studies of the Antioxidant Activity of Anthocyanins. *J. Food Sci. Technol. -Mysore* **2019**, *56*, 5518–5530. [[CrossRef](#)] [[PubMed](#)]
3. Correia, P.; Araújo, P.; Ribeiro, C.; Oliveira, H.; Pereira, A.R.; Mateus, N.; de Freitas, V.; Brás, N.F.; Gameiro, P.; Coelho, P.; et al. Anthocyanin-Related Pigments: Natural Allies for Skin Health Maintenance and Protection. *Antioxidants* **2021**, *10*, 1038. [[CrossRef](#)] [[PubMed](#)]
4. You, Y.; Yuan, X.; Liu, X.; Liang, C.; Zhan, J. Front Cover: Cyanidin-3-glucoside Increases Whole Body Energy Metabolism by Upregulating Brown Adipose Tissue Mitochondrial Function. *Mol. Nutr. Food Res.* **2017**, *61*, 1770111. [[CrossRef](#)]

5. Ng, T. Global, Regional, and National Prevalence of Overweight and Obesity in Children and Adults during 1980–2013: A Systematic Analysis for the Global Burden of Disease Study 2013. *Lancet* **2014**, *384*, 766–781. [[CrossRef](#)]
6. Al-Tahami, B.A.M.; Ismail, A.A.A.-S.; Bee, Y.T.G.; Awang, S.A.; Rani, W.R.S.W.A.; Sanip, Z.; Rasool, A.H.G. The effects of anti-obesity intervention with orlistat and sibutramine on microvascular endothelial function. *Clin. Hemorheol. Microcirc.* **2015**, *59*, 323–334. [[CrossRef](#)]
7. Siebenhofer, A.; Jeitler, K.; Horvath, K.; Berghold, A.; Semlitsch, T. Long-Term Effects of Weight-Reducing Drugs in People with Hypertension. *Cochrane Database Syst. Rev.* **2016**, *3*, CD007654. [[CrossRef](#)]
8. Cypess, A.M.; Chen, Y.C.; Sze, C.; Wang, K.; English, J.; Chan, O.; Holman, A.R.; Tal, M.; Palmer, M.R.; Kolodny, G.M. Cold but Not Sympathomimetics Activates Human Brown Adipose Tissue in Vivo. *Proc. Natl. Acad. Sci. USA* **2012**, *109*, 10001–10005. [[CrossRef](#)]
9. van Marken Lichtenbelt, W.D.; Vanhomerig, J.W.; Smulders, N.M.; Drossaerts, J.M.; Kemerink, G.J.; Bouvy, N.D.; Teule, G.J. None Cold-Activated Brown Adipose Tissue in Healthy Men. *N. Engl. J. Med.* **2009**, *360*, 1917. [[CrossRef](#)]
10. Villarroya, F.; Peyrou, M.; Giralt, M. Transcriptional Regulation of the Uncoupling Protein-1 Gene. *Biochimie* **2017**, *134*, 86–92. [[CrossRef](#)]
11. Escher, P.; Braissant, O.; Basu-Modak, S.; Michalik, L.; Wahli, W.; Desvergne, B. Wahli Rat PPARs: Quantitative Analysis in Adult Rat Tissues and Regulation in Fasting and Refeeding. *Endocrinology* **2001**, *142*, 4195–4202. [[CrossRef](#)]
12. Collins, S.; Yehuda-Shnaidman, E.; Wang, H. Positive and Negative Control of Ucp1 Gene Transcription and the Role of β -Adrenergic Signaling Networks. *Int. J. Obes.* **2010**, *34*, S28–S33. [[CrossRef](#)]
13. Harms, M.J.; Ishibashi, J.; Wang, W.; Lim, H.W.; Seale, P. Prdm16 Is Required for the Maintenance of Brown Adipocyte Identity and Function in Adult Mice. *Cell Metab.* **2014**, *19*, 593–604. [[CrossRef](#)] [[PubMed](#)]
14. Kajimura, S.; Seale, P.; Kubota, K.; Lunsford, E.; Frangioni, J.V.; Gygi, S.P.; Spiegelman, B.M. Initiation of Myoblast to Brown Fat Switch by a Prdm16–C/EBP- β Transcriptional Complex. *Nature* **2009**, *460*, 1154–1158. [[CrossRef](#)]
15. Matsukawa, T.; Inaguma, T.; Han, J.; Villareal, M.O.; Isoda, H. Cyanidin-3-Glucoside Derived from Black Soybeans Ameliorate Type 2 Diabetes through the Induction of Differentiation of Preadipocytes into Smaller and Insulin-Sensitive Adipocytes. *J. Nutr. Biochem.* **2015**, *26*, 860–867. [[CrossRef](#)] [[PubMed](#)]
16. Wu, T.; Yu, Z.; Tang, Q.; Song, H.; Gao, Z.; Chen, W.; Zheng, X. Honeysuckle Anthocyanin Supplementation Prevents Diet-Induced Obesity in C57BL/6 Mice. *Food Funct.* **2013**, *4*, 1654–1661. [[CrossRef](#)]
17. You, Y.; Liang, C.; Han, X.; Guo, J.; Ren, C.; Liu, G.; Huang, W.; Zhan, J. Mulberry Anthocyanins, Cyanidin 3-Glucoside and Cyanidin 3-Rutinoside, Increase the Quantity of Mitochondria during Brown Adipogenesis. *J. Funct. Foods* **2017**, *36*, 348–356. [[CrossRef](#)]
18. You, Y.; Han, X.; Guo, J.; Guo, Y.; Yin, M.; Liu, G.; Zhan, J. Cyanidin-3-Glucoside Attenuates High-Fat and High-Fructose Diet-Induced Obesity by Promoting the Thermogenic Capacity of Brown Adipose Tissue. *J. Funct. Foods* **2018**, *41*, 62–71. [[CrossRef](#)]
19. Becerril, S.; Gómez-Ambrosi, J.; Martín, M.; Moncada, R.; Frühbeck, G. Role of Prdm16 in the Activation of Brown Fat Programming. Relevance to the Development of Obesity. *Histol. Histopathol.* **2013**, *28*, 28. Available online: <http://hdl.handle.net/10201/61619> (accessed on 18 May 2021).
20. Hondares, E.; Rosell, M.; Diaz-Delfin, J.; Olmos, Y.; Monsalve, M.; Iglesias, R.; Villarroya, F.; Giralt, M. Peroxisome Proliferator-Activated Receptor α (PPAR α) Induces PPAR γ Coactivator 1 α (PGC-1 α) Gene Expression and Contributes to Thermogenic Activation of Brown Fat: Involvement of Prdm16. *J. Biol. Chem.* **2011**, *286*, 43112. [[CrossRef](#)]
21. Ohno, H.; Shinoda, K.; Ohyama, K.; Sharp, L.Z.; Kajimura, S. EHMT1 Controls Brown Adipose Cell Fate and Thermogenesis through the Prdm16 Complex. *Nature* **2013**, *504*, 163–167. [[CrossRef](#)]
22. Seale, P.; Kajimura, S.; Yang, W.; Chin, S.; Rohas, L.; Uldry, M.; Tavernier, G.; Langin, D.; Spiegelman, B. Transcriptional Control of Brown Fat Determination by Prdm16. *Cell Metab.* **2007**, *6*, 38–54. [[CrossRef](#)]
23. Cypess, A.M.; Lehman, S.; Williams, G.; Tal, I.; Rodman, D.; Goldfine, A.B.; Kuo, F.C.; Palmer, E.L.; Tseng, Y.H.; Doria, A. Identification and Importance of Brown Adipose Tissue in Adult Humans. *Obstet. Gynecol. Surv.* **2009**, *64*, 519–520. [[CrossRef](#)]
24. Himms-Hagen, J. Brown Adipose Tissue Thermogenesis: Interdisciplinary Studies. *Faseb. J.* **1990**, *4*, 2890–2898. [[CrossRef](#)] [[PubMed](#)]
25. Hidaka, S.; Kakuma, T.; Yoshimatsu, H.; Yasunaga, S.; Kurokawa, M.; Sakata, T. Molecular Cloning of Rat Uncoupling Protein 2 cDNA and Its Expression in Genetically Obese Zucker Fatty (Fa/Fa) Rats. *Biochim. Biophys. Acta* **1998**, *1389*, 178–186. [[CrossRef](#)]
26. Mao, W.; Yu, X.X.; Zhong, A.; Li, W.; Brush, J.; Sherwood, S.W.; Adams, S.H.; Pan, G. UCP4, a Novel Brain-Specific Mitochondrial Protein That Reduces Membrane Potential in Mammalian Cells. *FEBS Lett.* **1999**, *443*, 326–330. [[CrossRef](#)]
27. Solanes, G.; Vidal-Puig, A.; Grujic, D.; Flier, J.S.; Lowell, B.B. The Human Uncoupling Protein-3 Gene: Genomic structure, chromosomal localization, and genetic basis for short and long form transcripts *. *J. Biol. Chem.* **1997**, *272*, 25433–25436. [[CrossRef](#)]
28. Yu, X.X.; Mao, W.; Zhong, A.; Schow, P.; Brush, J.; Sherwood, S.W.; Adams, S.H.; Pan, G. Characterization of Novel UCP5/BMCP1 Isoforms and Differential Regulation of UCP4 and UCP5 Expression through Dietary or Temperature Manipulation. *Faseb. J. Off. Publ. Fed. Am. Soc. Exp. Biol.* **2000**, *14*, 1611. [[CrossRef](#)]
29. Rosen, E.; Spiegelman, B. What We Talk About When We Talk About Fat. *Cell* **2014**, *156*, 20–44. [[CrossRef](#)]
30. Rehnmark, S.; Bianco, A.C.; Kieffer, J.D.; Silva, J.E. Transcriptional and Posttranscriptional Mechanisms in Uncoupling Protein mRNA Response to Cold. *Am. J. Physiol.* **1992**, *262*, 58–67. [[CrossRef](#)] [[PubMed](#)]

31. You, Y.; Yuan, X.; Lee, H.J.; Huang, W.; Jin, W.; Zhan, J. Zhan Mulberry and Mulberry Wine Extract Increase the Number of Mitochondria during Brown Adipogenesis. *Food Funct.* **2015**, *6*, 401–408. [[CrossRef](#)]
32. Han, X.; Guo, J.; You, Y.; Yin, M.; Liang, J.; Ren, C.; Huang, W. Vanillic Acid Activates Thermogenesis in Brown and White Adipose Tissue. *Food Funct.* **2018**, *9*, 4366–4375. [[CrossRef](#)]
33. Han, X.; Zhang, Y.; Guo, J.; You, Y.; Huang, W. Chlorogenic Acid Stimulates the Thermogenesis of Brown Adipocytes by Promoting the Uptake of Glucose and the Function of Mitochondria. *J. Food Sci.* **2019**, *84*, 3815–3824. [[CrossRef](#)]
34. Echtay, K. Mitochondrial Uncoupling Proteins—What Is Their Physiological Role? *Free Radic. Biol. Med.* **2007**, *43*, 1351–1371. [[CrossRef](#)]
35. Jastroch, M.; Withers, K.; Klingenspor, M. Klingenspor Uncoupling Protein 2 and 3 in Marsupials: Identification, Phylogeny, and Gene Expression in Response to Cold and Fasting in *Antechinus Flavipes*. *Physiol. Genom.* **2004**, *17*, 130–139. [[CrossRef](#)] [[PubMed](#)]
36. Collins, S.; Daniel, K.W.; Petro, A.E.; Surwit, R.S. Strain-Specific Response to Beta 3-Adrenergic Receptor Agonist Treatment of Diet-Induced Obesity in Mice. *Endocrinology* **1997**, *138*, 405–413. [[CrossRef](#)] [[PubMed](#)]
37. Kumar, M. Differential Effects of Retinoic Acid on Uncoupling Protein-1 and Leptin Gene Expression. *J. Endocrinol.* **1998**, *157*, 237–243. [[CrossRef](#)] [[PubMed](#)]
38. Rabelo, R.; Camirand, A.; Silva, J.E. Silva 3',5'-Cyclic Adenosine Monophosphate-Response Sequences of the Uncoupling Protein Gene Are Sequentially Recruited during Darglitazone-Induced Brown Adipocyte Differentiation. *Endocrinology* **1997**, *138*, 5325–5332. [[CrossRef](#)]
39. Sasaki, N.; Uchida, E.; Niiyama, M.; Yoshida, T.; Saito, M. Anti-Obesity Effects of Selective Agonists to the Beta 3-Adrenergic Receptor in Dogs. II. Recruitment of Thermogenic Brown Adipocytes and Reduction of Adiposity after Chronic Treatment with a Beta 3-Adrenergic Agonist. *J. Vet. Med. Sci.* **1998**, *60*, 465. [[CrossRef](#)]
40. Savontaus, E.; Rouru, J.; Boss, O.; Huupponen, R.; Koulu, M. Differential Regulation of Uncoupling Proteins by Chronic Treatments with Beta 3-Adrenergic Agonist BRL 35135 and Metformin in Obese Fa/Fa Zucker Rats. *Biochem. Biophys. Res. Commun.* **1998**, *246*, 899–904. [[CrossRef](#)] [[PubMed](#)]
41. Kang, S.; Bajnok, L.; Longo, K.A.; Petersen, R.K.; Hansen, J.B.; Kristiansen, K.; Macdougald, O.A. Effects of Wnt Signaling on Brown Adipocyte Differentiation and Metabolism Mediated by PGC-1 α . *Mol. Cell. Biol.* **2005**, *25*, 1272–1282. [[CrossRef](#)]
42. Seale, P.; Conroe, H.M.; Estall, J.; Kajimura, S.; Frontini, A.; Ishibashi, J.; Cohen, P.; Cinti, S.; Spiegelman, B.M. Prdm16 Determines the Thermogenic Program of Subcutaneous White Adipose Tissue in Mice. *J. Clin. Investig.* **2011**, *121*, 96–105. [[CrossRef](#)]
43. Ricquier, D.; Casteilla, L.; Bouillaud, F. Molecular Studies of the Uncoupling Protein. *FASEB J.* **1991**, *5*, 2237–2242. [[CrossRef](#)] [[PubMed](#)]
44. Seale, P.; Bjork, B.; Yang, W.; Kajimura, S.; Chin, S.; Kuang, S.; Scimè, A.; Devarakonda, S.; Conroe, H.M.; Erdjument-Bromage, H.; et al. Prdm16 Controls a Brown Fat/Skeletal Muscle Switch. *Nature* **2008**, *454*, 961–967. [[CrossRef](#)] [[PubMed](#)]
45. Wang, L.; Zhan, J.; Huang, W. Grape Seed Proanthocyanidins Induce Apoptosis and Cell Cycle Arrest of HepG2 Cells Accompanied by Induction of the MAPK Pathway and NAG-1. *Antioxidants* **2020**, *9*, 1200. [[CrossRef](#)] [[PubMed](#)]
46. Kay, C.D.; Kroon, P.A.; Cassidy, A. The Bioactivity of Dietary Anthocyanins Is Likely to Be Mediated by Their Degradation Products. *Mol. Nutr. Food Res.* **2010**, *53*, 92–101. [[CrossRef](#)]
47. Pace, E.; Jiang, Y.; Clemens, A.; Crossman, T.; Rupasinghe, H.V. Impact of Thermal Degradation of Cyanidin-3-O-glucoside of Haskap Berry on Cytotoxicity of Hepatocellular Carcinoma HepG2 and Breast Cancer MDA-MB-231 Cells. *Antioxidants* **2018**, *7*, 24. [[CrossRef](#)]